AIAA Journal
Vol. 42, No. 12, December 2004

Technical Notes

TECHNICAL NOTES are short manuscripts describing new developments or important results of a preliminary nature. These Notes cannot exceed six manuscript pages and three figures; a page of text may be substituted for a figure and vice versa. After informal review by the editors, they may be published within a few months of the date of receipt. Style requirements are the same as for regular contributions (see inside back cover).

Solving Magnetohydrodynamic Equations Without Special Treatment for Divergence-Free Magnetic Field

Moujin Zhang* and S.-T. John Yu†
The Ohio State University, Columbus, Ohio 43202
Shan-Chuen Lin‡
Wayne State University, Detroit, Michigan 48202
and
Sin-Chung Chang§ and Isaiah Blankson¶
NASA John H. Glenn Research Center at Lewis Field, Cleveland, Ohio 44135

I. Introduction

RECENTLY, computational magnetohydrodynamics (MHD) has drawn attention as a result of growing interests in plasma-based aerodynamics, including flow manipulation through plasma, onboard power generation, and drag reduction in hypersonic vehicles. Because plasma flows are much more complex than the regular gas dynamics, extension of the existing computational-fluid-dynamics methods for solving the plasma equations involves unique requirements and poses a greater challenge. A critical issue in computational MHD is to maintain the divergence-free condition for the magnetic field, that is, $\nabla \cdot \boldsymbol{B} = 0$, for all time and at all locations in the computational domain. Analytically, this constraint is ensured if it is satisfied in the initial condition. However, it is difficult to maintain the constraint in numerical calculations. Violating the $\nabla \cdot \boldsymbol{B} = 0$ constraint might allow numerical errors to be accumulated, leading to erroneous solutions and/or numerical instability. Usually, a special treatment is used to enforce the constraint. These procedures can be categorized into three groups: 1) the projection procedure reported by Brackbill and Barnes,[1] 2) the eight-wave formulation reported by Powell,[2] and 3) the constrained transport procedures reported by Evans and Hawley,[3] Dai and Woodward,[4] Ryu et al.,[5] and Balsara and Spice.[6] Toth[7] has compared and assessed these popular methods.

Received 23 February 2004; revision received 28 July 2004; accepted for publication 28 July 2004.

*Research Associate, Mechanical Engineering Department; zhang.493@osu.edu. Member AIAA.
†Associate Professor, Mechanical Engineering Department, 650 Ackerman Road, Suite 255; yu.274@osu.edu. Member AIAA.
‡Ph.D. Student, Mechanical Engineering Department; currently Senior Project Engineer, Structures and Closures Vehicle System Department, General Motors Corp., Warren, MI 48090; ad5516@wayne.edu.
§Senior Aerospace Scientist; sin-chung.chang@lerc.nasa.gov. Member AIAA.
¶Senior Technologist; isaiah.blankson@lerc.nasa.gov. Member AIAA.

Because of the complexity of the plasma problems, a highly accurate but simple numerical method is desirable. Simplicity is particularly important for further extending the solvers to model plasma processes involving multiple components and chemical reactions. To this end, we propose to use the space-time conservation element and solution element (CESE) method for computational MHD. We will demonstrate the capability of the CESE method by solving two standard MHD problems: 1) a rotated shock-tube problem by Brio and Wu[8] and 2) a vortex problem by Orszag and Tang.[9] In the first case, a two-dimensional calculation is conducted on a rotated coordinate frame for solving an essentially one-dimensional process. Direct comparison between the two-dimensional result with the corresponding one-dimensional solution allows us to assess the numerical accuracy of the CESE method in maintaining the $\nabla \cdot \boldsymbol{B} = 0$ constraint. For this calculation, we do not impose any special treatment for the constraint. In the second case, we conduct the two-dimensional calculations with and without imposing the constraint by a projection method. For both calculations, the results compare well with the previously published solution. For this particular case, we show that the projection method does not improve the quality of the solution.

II. Governing Equations and the CESE Method

The ideal MHD equations in two spatial dimensions can be expressed as

$$\frac{\partial \boldsymbol{U}}{\partial t} + \frac{\partial \boldsymbol{F}}{\partial x} + \frac{\partial \boldsymbol{G}}{\partial y} = 0 \tag{1}$$

where

$$\boldsymbol{U} = (\rho, \rho u, \rho v, \rho w, e, B_x, B_y, B_z)^T = (u_1, u_2, u_3, \ldots, u_8)^T \tag{2}$$

$$\begin{aligned}\boldsymbol{F} = \big[&\rho u, \rho u^2 + p_0 - B_x^2, \rho u v - B_x B_y, \rho u w - B_x B_z, (e + p_0)u \\ &- B_x(u B_x + v B_y + w B_z), 0, u B_y - v B_x, u B_z - w B_x\big]^T \\ = (&f_1, f_2, f_3, f_4, f_5, f_6, f_7, f_8)^T\end{aligned} \tag{3}$$

$$\begin{aligned}G = \big[&\rho v, \rho v u - B_y B_x, \rho v^2 + p_0 - B_y^2, \rho v w - B_y B_z, (e + p_0)v \\ &- B_y(u B_x + v B_y + w B_z), v B_x - u B_y, 0, v B_z - w B_y\big]^T \\ = (&g_1, g_2, g_3, g_4, g_5, g_6, g_7, g_8)^T\end{aligned} \tag{4}$$

In the preceding equations, ρ and p and e are the density and pressure; u, v, and w are velocity components in x, y, and z directions, respectively. B_x, B_y, and B_z are magnetic filed components in the x, y, and z directions; p_0 is the total pressure and defined as $p_0 = p + (B_x^2 + B_y^2 + B_z^2)/2$; and e is the specific total energy and is defined as $e = \rho\varepsilon + \rho(u^2 + v^2 + w^2)/2 + (B_x^2 + B_y^2 + B_z^2)/2$. For calorically ideal gases, the specific internal energy ε is defined as $\varepsilon = p/(\gamma - 1)\rho$, in which γ is the specific heat ratio. In addition to the preceding equations, initial condition of magnetic field $\boldsymbol{B}$ must satisfy the divergence-free constraint, $\nabla \cdot \boldsymbol{B} = 0$.

To solve Eq. (1) by the CESE method, let $x_1 = x$, $x_2 = y$, and $x_3 = t$ be the coordinates of a three-dimensional Euclidean space E_3. Equation (1) becomes a divergence-free condition:

$$\nabla \cdot \boldsymbol{h}_m = 0 \tag{5}$$

where $\boldsymbol{h}_m = (f_m, g_m, u_m)$, $m = 1, 2, \ldots, 8$, is space-time vector in E_3. By Gauss's divergence theorem, we have

$$\int_V \nabla \cdot \boldsymbol{h}_m \, \mathrm{d}V = \oint_{S(V)} \boldsymbol{h}_m \cdot \mathrm{d}\boldsymbol{s} = 0 \tag{6}$$

where $S(V)$ is the boundary of an arbitrary space-time region V in E_3 and $\mathrm{d}\boldsymbol{s} = \boldsymbol{n}\,\mathrm{d}\sigma$, where $\mathrm{d}\sigma$ and $\boldsymbol{n}$ are the area and the outward unit normal vector of a surface element on $S(V)$. We use the CESE method to integrate Eq. (3) in the space-time domain. Details of the CESE methods have been extensively illustrated in the cited references.[10–15] In what follows, we provide brief comments on unique features of the method.

The tenet of the CESE method is to treat space and time as one entity to obtain an explicit time-march scheme based on space-time flux balance. Separated definitions of conservation element (CE) and solution element (SE) are used. Inside a SE, the flow variables are assumed continuous and can be represented by a predetermined function. Over a CE, flux conservation is enforced, and the values of flow variables could be discontinuous. Time marching is carried out in a leapfrog fashion such that across each cell interface of neighboring SEs flow information propagates in only one direction, that is, toward the future. The mathematical formulation used in the CESE method involves only a first-order Taylor-series expansion and simple reweighting algorithms. The construction of CE and SE for the MHD equations is identical to that illustrated in Ref. 14.

III. Results and Discussion

A. Rotated Shock-Tube Problem

To test the capabilities of the numerical algorithm for maintaining the $\nabla \cdot \boldsymbol{B} = 0$ constraint for flows in multidimensions, a common practice, as reported by Toth[7] and Jiang and Wu,[16] is to perform two-dimensional calculation of a rotated one-dimensional problem. Referring to Fig. 1, the computation is conducted in domain OABC in x–y coordinates. The one-dimensional problem is defined along the ξ axis. Through coordinate transformation, the flow variables in the x–y coordinates can be obtained from those in the ξ–η coordinates and vice versa. Because the one-dimensional solution would automatically satisfy $\nabla \cdot \boldsymbol{B} = 0$, the net effect of violating the $\nabla \cdot \boldsymbol{B} = 0$ constraint in the two-dimensional results can be straightforwardly judged by direct comparison between the two-dimensional result with the corresponding one-dimensional one. Here, the Brio and Wu's shock-tube problem[8] is employed for the purpose.

The present calculation is similar to that reported by Jiang and Wu.[16] The computational domain is $(x, y) \in \lfloor 0, \sqrt{2}/2 \rfloor \times \lfloor 0, \sqrt{2}/2 \rfloor$. The rotated angle φ between the x-y system and the ξ-η system is 45 deg. The initial jump condition is prescribed along the ξ axis:

$$(\rho, u, v, w, p, B_\eta, B_z) = \begin{cases} (1.000, 0, 0, 0, 1.0, +1, 0) & \text{for} \quad \xi < 0.5 \\ (0.125, 0, 0, 0, 0.1, -1, 0) & \text{for} \quad \xi > 0.5 \end{cases}$$

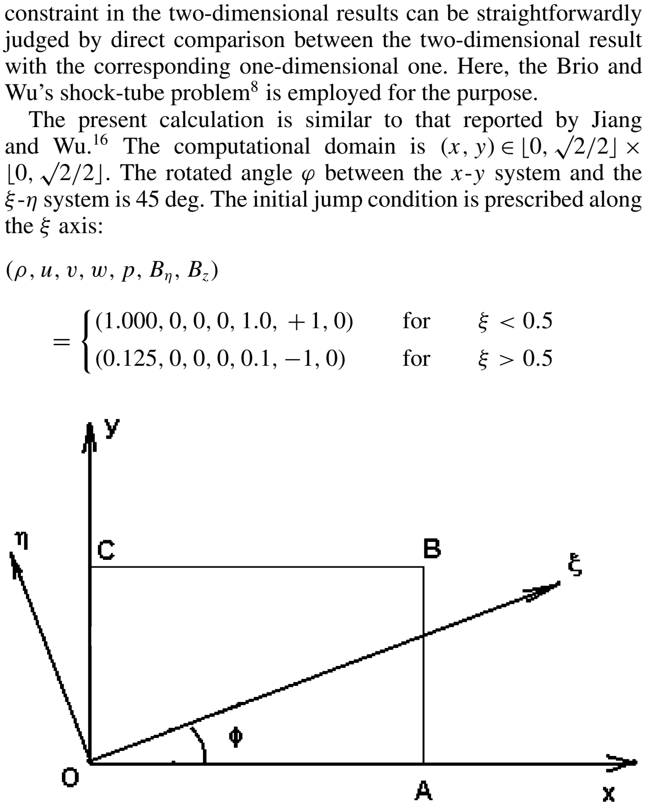

Fig. 1 Relation between x–y coordinates and ξ–η coordinates.

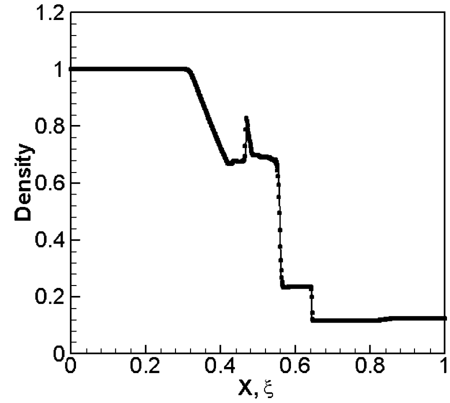

Fig. 2 Density profile of rotated Brio and Wu's problem: ——, data provided in Ref. 8.

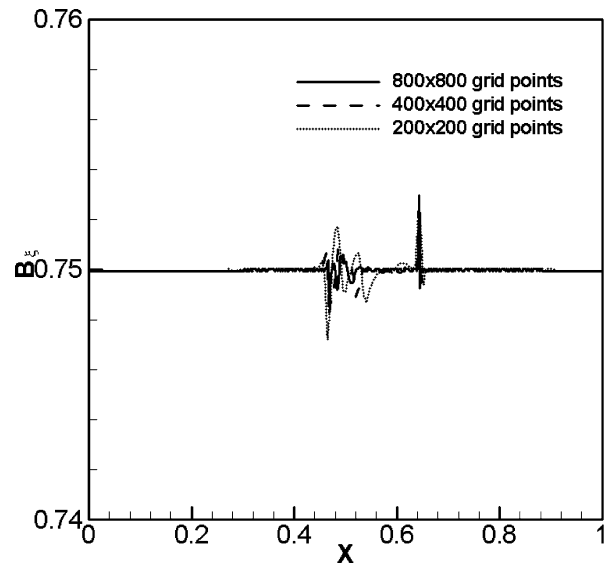

Fig. 3 B_ξ profile of rotated Brio and Wu's problem with different resolution.

with $\gamma = 2$ and $B_\xi = 0.75$. Figure 2 shows the profile of density at $t = 0.1$, in which the solid line is a one-dimensional result by Brio and Wu[8] and dots are our two-dimensional result by using the CESE method. The mesh density is 800×800.

Figure 3 shows the two-dimensional solution of B_ξ along the ξ axis at time $t = 0.1$. Analytically, $B_\xi = 0.75$ along the ξ axis, that is, the initial condition, during the flow evolution. Oscillations occur around discontinuities. Away from flow discontinuities, B_ξ maintains constant. Figure 3 also shows results with two other meshes: 200×200 and 400×400. Coarser meshes have limited influence on the $\nabla \cdot \boldsymbol{B} = 0$ condition. Note that similar oscillations of B_ξ also appeared in Jiang and Wu's two-dimensional results.[16] They used a high-order weighted essentially nonoscillatory (WENO) scheme in conjunction with a projection procedure for $\nabla \cdot \boldsymbol{B} = 0$. The magnitude of the oscillations in B_ξ in our two-dimensional results is comparable to that reported by Jiang and Wu.[16] The use of the projection procedure in Jiang and Wu's calculation is critical to their result. Without the special treatment, significant spurious oscillations occur. In our case, no spurious oscillation occurs, and no special treatment is used.

B. MHD Vortex

The initial condition of Orszag and Tang's problem[9] is

$$\rho(x, y, 0) = \gamma^2, \qquad p(x, y, 0) = \gamma$$

$$u(x, y, 0) = -\sin y, \qquad v(x, y, 0) = \sin x, \qquad w(x, y, 0) = 0$$

$$B_x(x, y, 0) = -\sin y, \qquad B_y(x, y, 0) = \sin 2x, \qquad B_z(x, y, 0) = 0$$

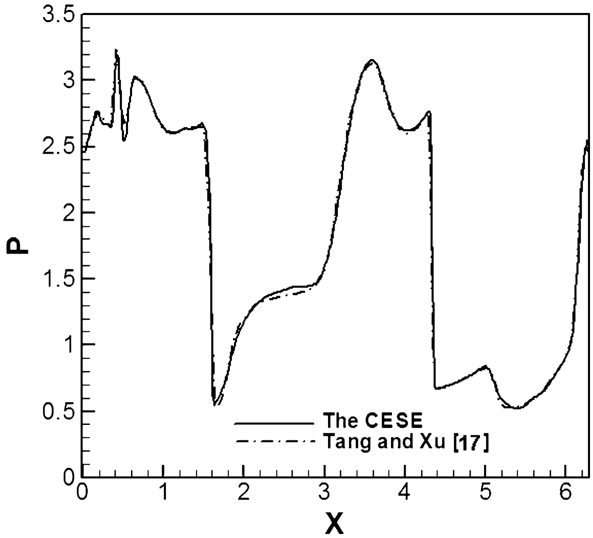

Fig. 4 Pressure profile along $y = 0.625\pi$ at $t = 3$ of Orszag and Tang's problem.

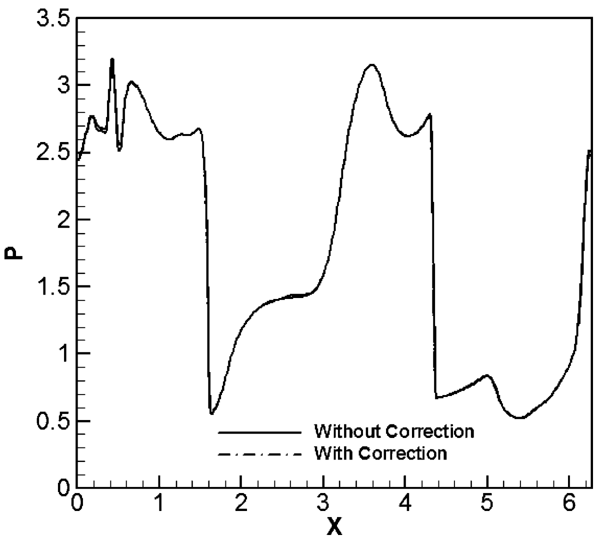

Fig. 5 Comparison between the CESE method with and without a projection procedure for keeping $\nabla \cdot \boldsymbol{B} = 0$.

The computational domain is $[0, 2\pi] \times [0, 2\pi]$, which is discretized by 193×193 grid nodes. Periodic boundary conditions are employed on the two lateral boundaries and the top and bottom boundaries. We ran the calculation from $t = 0$ to 10. Figure 4 shows the comparison between our calculated pressure profile along line $y = 0.625\pi$ at $t = 3$, with that reported by Tang and Xu[17] (also private communication, 2004), in which a high-order gas-kinetic method coupled with a projection procedure was used to solve the same problem. Our result is almost identical to that reported by Tang and Xu[17] (also, private communication, 2004).

To assess the effect of the projection procedure in maintaining $\nabla \cdot \boldsymbol{B} = 0$ on the CESE's results, we repeat the same calculation by employing the projection procedure in our solver. At every time step, we solve a Poisson equation $\nabla^2\phi + \nabla \cdot \boldsymbol{B} = 0$, with $\boldsymbol{B}$ obtained by the CESE method. We then correct magnetic field as $\boldsymbol{B}^c = \nabla\phi + \boldsymbol{B}$, for which $\nabla \cdot \boldsymbol{B}^c = 0$. The divergence-free $\boldsymbol{B}^c$ is used for the solution at the next time step. Figure 5 shows the comparison between the pressure profiles along line $y = 0.625\pi$ at $t = 3$ with and without using the projection method. No obvious difference is observed.

IV. Conclusions

In this Note, we report the extension of the conservation element and solution element (CESE) method for solving the magnetohydrodynamics (MHD) equations in two spatial dimensions. Two benchmark problems are calculated: 1) a rotated one-dimensional shock-tube problem proposed by Brio and Wu[8] and 2) a MHD vortex problem proposed by Orszag and Tang.[9] In both cases, numerical results by the CESE method without using any special treatment for $\nabla \cdot \boldsymbol{B} = 0$ compare favorably with previously reported results. To further assess the numerical solution, we couple the projection procedure for $\nabla \cdot \boldsymbol{B} = 0$ with the CESE solver and recalculate Tang and Orszag's problem. The result shows no improvement. Moreover, applications of the CESE method to these two MHD problems without any special treatment for $\nabla \cdot \boldsymbol{B} = 0$ show no numerical instability in calculations.

References

[1]Brackbill, J. P., and Barnes, D. C., "The Effect of Nonzero $\nabla \cdot \boldsymbol{B}$ on the Numerical Solution of the Magnetohydrodynamic Equations," *Journal of Computational Physics*, Vol. 35, No. 2, 1980, pp. 426–430.

[2]Powell, K. G., "An Approximate Riemann Solver for Magneto-Hydro-Dynamics," ICASE Rept. 94-24, April 1994.

[3]Evans, C. R., and Hawley, J. F., "Simulation of Magnetohydrodynamic Flows: A Constrained Transport Method," *Astrophysics Journal*, Vol. 332, No. 2, 1988, pp. 659–677.

[4]Dai, W., and Woodward, P. R., "A Simple Finite Difference Scheme for Multidimensional Magnetohydrodanamical Equations," *Journal of Computational Physics*, Vol. 142, No. 2, 1998, pp. 331–369.

[5]Ryu, D., Miniati, F., Jones, T. W., and Frank, A., "A Divergence-Free Upwind Code for Multidimensional Magnetohydrodynamic Flows," *Astrophysics Journal*, Vol. 509, No. 1, 1998, pp. 244–255.

[6]Balsara, D. S., and Spice, D. S., "A Staggered Mesh Algorithm Using High Order Godunov Fluxes to Ensure Solenoidal Magnetic Fields in Magnetohydrodynamic Simulations," *Journal of Computational Physics*, Vol. 149, No. 1, 1999, pp. 270–292.

[7]Tóth, G., "The Constraint $\nabla \cdot \boldsymbol{B} = 0$ in Shock Capturing Magnetohydrodynamics Codes," *Journal of Computational Physics*, Vol. 161, No. 2, 2000, pp. 605–652.

[8]Brio, M., and Wu, C. C., "An Upwind Differencing Scheme for the Equations of Ideal Magnetohydrodynamics," *Journal of Computational Physics*, Vol. 75, No. 2, 1988, pp. 400–422.

[9]Orszag, A., and Tang, C. M., "Small-Scale Structure of Two-Dimensional Magnetohydrodynamic Turbulence," *Journal of Fluid Mechanics*, Vol. 90, 1979, pp. 129–145.

[10]Chang, S. C., and To, W. M., "A New Numerical Framework for Solving Conservation Laws—The Method of Space-Time Conservation Element and Solution Element," NASA TM 104498, Aug. 1991.

[11]Chang, S. C., "The Method of Space-Time Conservation Element and Solution Element—A New Approach for Solving the Navier–Stokes and the Euler Equations," *Journal of Computational Physics*, Vol. 119, No. 2, 1995, pp. 295–324.

[12]Chang, S. C., Wang, X. Y., and Chow, C. Y., "The Space-Time Conservation Element and Solution Element Method: A New High-Resolution and Genuinely Multidimensional Paradigm for Solving Conservation Laws," *Journal of Computational Physics*, Vol. 156, No. 1, 1999, pp. 89–136.

[13]Wang, X. Y., and Chang, S. C., "A 2D Non-Splitting Unstructured Triangular Mesh Euler Solver Based on the Space-Time Conservation Element and Solution Element Method," *Computational Fluid Dynamics Journal*, Vol. 8, No. 2, 1999, pp. 309–325.

[14]Zhang, Z. C., Yu, S. T., and Chang, S. C., "A Space-Time Conservation Element and Solution Element Method for Solving the Two- and Three-Dimensional Unsteady Euler Equations Using Quadrilateral and Hexahedral Meshes," *Journal of Computational Physics*, Vol. 175, No. 1, 2002, pp. 168–199.

[15]Zhang, M. J., Lin, S. C., Yu, S. T., Chang, S. C., and Blankson, I., "Application of the Space-Time Conservation Element and Solution Element Method to the Ideal Magnetohydrodynamics Equations," AIAA Paper 2002-3888, July 2002.

[16]Jiang, G.-S., and Wu, C. C., "A High-Order WENO Finite Difference Scheme for the Equations of Ideal Magnetohydrodynamics," *Journal of Computational Physics*, Vol. 150, No. 2, 1999, pp. 561–594.

[17]Tang, H.-Z., and Xu, K., "A High-Order Gas-Kinetic Method for Multidimensional Ideal Magnetohydrodynamics," *Journal of Computational Physics*, Vol. 165, No. 1, 2000, pp. 69–88.

D. Gaitonde
Associate Editor